J. Mt. Sci. (2019) 16(11): 2605-2614 e-mail: jms@imde.ac.cn http://jms.imde.ac.cn
https://doi.org/10.1007/s11629-019-5514-8

Spatial distribution of the oxygen-18 in precipitation in China based on a new empirical model

ZHAO Pei[1,2] https://doi.org/0000-0003-2350-3025; e-mail: pzhaosl@yeah.net

GUO Zheng-sheng[3] https://doi.org/0000-0001-7943-0377; e-mail:1452952176@qq.com

SHE Dong-li[4] https://doi.org/0000-0002-0612-4325; e-mail: shedongli@hhu.edu.cn

TANG Xiang-yu[2*] https://doi.org/0000-0003-0467-9180; e-mail: xytang@imde.ac.cn

**Corresponding author*

1 Department of Geography, Shangluo University, Shangluo 726000, China

2 Key Laboratory of Mountain Surface Processes and Ecological Regulation, Institute of Mountain Hazards and Environment, Chinese Academy of Sciences, Chengdu 610041, China

3 College of Urban and Environment Sciences, Shanxi Normal University, Linfen 041000, China

4 State Key Laboratory of Soil Erosion and Dryland Farming on the Loess Plateau, Research Center of Soil and Water Conservation and Ecological Environment, Chinese Academy of Sciences & Ministry of Education, Yangling 712100, China

Citation: Zhao P, Guo ZS, She DL, et al. (2019) Spatial distribution of the oxygen-18 in precipitation in China based on a new empirical model. Journal of Mountain Science 16(11). https://doi.org/10.1007/s11629-019-5514-8

Abstract: Modeling the oxygen-18 in precipitation based on regional topography and meteorological factors is helpful to constrain missing isotopic data in some regions that is required for many paleoclimate, eco-hydrological and atmospheric circulation studies. Therefore, the relationship between δ^{18}O in precipitation ($\delta^{18}O_{PPT}$) and the affecting factors need to be thoroughly understood. We present a model considering the combined effects of temperature, altitude, and latitude on the spatial variability of annual average of stable isotopes in precipitation across China. This new model performed significantly better (P<0.05) than the widely used Farquhar and Bowen & Wilkinson models. Our model allows modelling the spatial distribution of isotopes in precipitation depending on temperature variation. The residuals of presented model did not significantly correlate with altitude. Based on the model and residuals, a high-resolution map of annual average $\delta^{18}O_{ppt}$ across China was generated. $\delta^{18}O_{PPT}$ decreased from low toward high latitudes and from low towards high altitudes area. The model application provides important information for ancient climate, hydrological cycle and water vapor sources studies.

Keywords: Climate change; Isotope hydrology; Geographic information; Spatial distribution

Received: 11-Apr-2019
Revised: 14-Jul-2019
Accepted: 25-Jul-2019

Introduction

The oxygen-18 in precipitation as recorded in some oxygenated natural materials has been used in studies of ancient and modern process of global and regional climatic conditions and hydrological processes (Zhang & Yao 1994; Bowen & Wilkinson 2002; Chan et al. 2012; Terzer et al. 2013; Zhang et al. 2017). Oxygen-18 in precipitation was used as a natural tracer to reconstruct paleohydrology or/and paleoclimate based on isotopic composition of the natural materials, such as glacial ice (Petit et al. 1999), groundwater (Dutton 1995), fossil enamel (Sharp & Cerling 1998), and tree rings (Liu et al. 2008). These records are frequently used to estimate paleo-temperature that is based on the strong spatial and temporal correlation between $\delta^{18}O$ in precipitation ($\delta^{18}O_{PPT}$) and local temperature (Dansgaard 1964; Fricke & O'Neil 1999).

In addition, if the records in the materials are not subsequently altered, they can be used to estimate their geographical origin according to the water isotopic compositions. Many disciplines such as archaeology, ecology, anthropology, and forensic science are of interest in such applications (West et al. 2010). However, application of $\delta^{18}O$ as a tracer in these studies, needs spatially high resolution data on isotopes in modern precipitation (Ma et al. 2018). This means that the mapped information can compare with the proxy data for paleo-precipitation as a spatial reference (Bowen & Wilkinson 2002). In addition, West et al. (2010) and Bowen (2010) argued that the spatial information on isotopic composition in precipitation is helpful to gain insights of the past (e.g., Ufnar et al. 2004; Schmidt et al. 2007) and present (e.g., Salati et al. 1979; Gat et al. 2003) large-scale water cycle process. For instance, in large-scale hydrological studies, spatial pattern of isotope ratios in precipitation are of important to partition the water source of large rivers (Bowen et al. 2008; West et al. 2010). However, the number of monitoring stations of $\delta^{18}O_{PPT}$ are limited and unevenly distributed across the globe. For example, there are only few isotopic datasets of precipitation in high-altitude (e.g. Siberia) and desert regions (e.g. Takla Makan Desert). Thus, the application of $\delta^{18}O$ as a tracer in hydrological cycle is restricted to particular regions.

Estimations of $\delta^{18}O_{PPT}$ at a given location is often derived from interpolation between Global Network of Isotopes in Precipitation (GNIP) stations (Terzer et al. 2013) or by reference to the nearest station. However, the oxygen-18 in precipitation is controlled by Rayleigh distillation of atmospheric vapor, primarily by change in air-mass temperature (Rozanski et al. 1992). Interpolation methods ignore the geographic parameters and highly depend on the number of stations (Bowen & Wilkinson 2002). Reasonably accurate and low resolution maps of $\delta^{18}O_{PPT}$ were estimated by coupling with global circulation models (GCM) (Hoffmann & Heimann 1997). Nevertheless, the limited knowledge of relevant meteorological parameters, complex calculations and uncertainties regarding the GCM results to the past climate limited the application of such theoretical models to paleo-$\delta^{18}O_{PPT}$ proxy data (Bowen & Wilkinson 2002). Beyond that, Farquhar et al. (1993) developed a global map of precipitation isotope ratios using meteorological and geographical variables in order to estimate the transfer of $\delta^{18}O$ from leaf water to atmospheric CO_2. However, this model had 6 parameters which was relative complex. After that, Bowen & Wilkinson (2002) developed another empirical model (Bowen & Wilkinson model, BW model) related to latitude and altitude to describe the spatial distribution of $\delta^{18}O$ for global meteoric precipitation. Based on these models, the relationships between geographical parameters and $\delta^{18}O_{PPT}$ on a regional scale (Liu et al. 2008) and global scale (Bowen & Wilkinson 2002) have been addressed. Lykoudis & Argiriou (2007) proposed that statistical models of the isotopic composition of precipitation using meteorological parameters show better goodness of fit than those using only geographical data. Nevertheless, the BW model proposed by Bowen & Wilkinson (2002) produced the best result on an annual basis.

Bowen (2008) stated that "overwhelming dominance of temperature- and precipitation amount-related isotopic seasonality within specific, well-defined geographic zones and indicate that these zones encompass most of Earth's continental land surface." Thus, the important role of meteorological factors should not be neglected when simulating precipitation isotopic composition. At a defined location, altitude and latitude are fixed over considered time scales. This implies that $\delta^{18}O_{PPT}$ derived with BW model limited to these variables is also fixed over time. Therefore, BW model accounted for the geographical parameters in controlling the distribution of $\delta^{18}O_{PPT}$, but not illuminate the effects of meteorological parameters on the past changes of $\delta^{18}O_{PPT}$. Terzer et al. (2013) noted that the present precipitation isotope mapping products had an inherent assumption of temporal constancy over the study period. In fact, spatial variation of $\delta^{18}O_{PPT}$ is an integrated result of these geographic and meteorological factors.

Here we aimed to develop a high-resolution map of $\delta^{18}O_{PPT}$ across China based on an empirically derived model incorporating basic geographic parameters and meteorological variables such as temperature, altitude, and latitude. The objectives of this research are: (1) to generate a higher-resolution map of average annual $\delta^{18}O_{PPT}$ in China based on this model; (2) to find out the distribution pattern of the $\delta^{18}O_{PPT}$ across China.

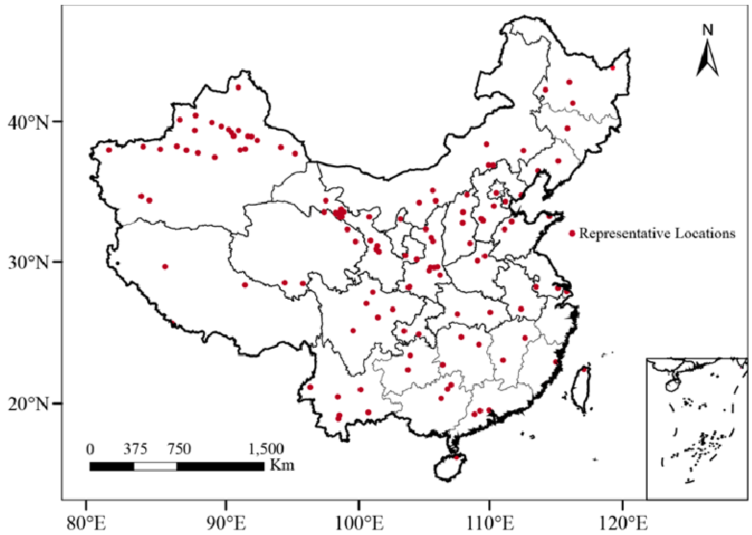

Figure 1 The distribution of the 126 stations across China, where $\delta^{18}O_{PPT}$ was sampled.

1 Data Source and Methods

The analysis is based on the annual weighted $\delta^{18}O_{PPT}$ data. The ratio $^{18}O/^{16}O$ in a sample is expressed in per mil (‰) in the δ-notation relative to V-SMOW (Vienna Standard Mean Ocean Water). The data on $\delta^{18}O_{PPT}$ was mainly derived from the International Atomic Energy Agency-World Meteorological Organization Global Network for Isotopes in Precipitation (GNIP) database (http://isohis.iaca.org), and from published data (Zhang 1989; Gao 1993; Wei & Lin 1994; Cai 2000; Wang et al. 2001; Tian et al. 2003; Tu et al. 2004; Zhang et al. 2006; Liu et al. 2007; Tian et al. 2007; Liu et al. 2009; Zhao et al. 2011; Wu et al. 2011; Wang et al. 2012; Chen et al. 2013; Ma et al. 2013; Yang et al. 2014; Pang et al. 2015; Guo et al. 2015; Wang et al. 2016), and from our measurements in Yanting and Shangluo (not published data). $\delta^{18}O_{PPT}$ values were available for 126 locations in total and their spatial distributions across China are shown in Figure 1.

For each station, the latitude, elevations, annual average temperature of the sites were reported. A digital elevation model (DEM) of 5 km resolution was obtained from the GTOPO30 (US National Geographic Data Center 1998) to get altitude and latitude values for each station. For those stations, the altitude ranges from 3 to 5200 m a.s.l.. The annual average temperature was taken from 824 meteorological stations (available at http://data.cma.cn). Most considered values of $\delta^{18}O_{PPT}$ were amount-weighted averages for one or more complete years, calculated as follows

$$\overline{\delta^{18}O} = \sum P_i \delta^{18}O_i \Big/ \sum P_i \qquad (1)$$

where P_i and $\delta^{18}O_i$ denote the precipitation amount and corresponding oxygen isotope value, respectively. Amount-weighted average values were calculated for each station. However, for some sites only the average, non-weighted values were provided in the literature. To test the potential biased introduced by average, we compared the average values to the weighted average values where possible. The average annual $\delta^{18}O_{PPT}$ values did not produce result significantly different from the weighted averages (results not shown). Bowen & Wilkinson (2002) also reported the same result in a global dataset.

We tested the model by Farquhar et al. (1993), who were among the first to create a global map of precipitation isotope ratios using ancillary (i.e. other than spatial position) variables. They developed a multiregression model according to the following relationship:

$$\delta^{18}O = aT + bT^2 + cPPT + dPPT^2 + eALT^{0.5} + f \qquad (2)$$

where $\delta^{18}O_{PPT}$ is an initial estimate of average annual value of oxygen isotope compositions of precipitation, T is the average annual temperature (°C), PPT is the annual precipitation (mm), and ALT is altitude (m) and a, b, c, d, e and f are empirical parameters.

In addition, we tested the BW model proposed by Bowen & Wilkinson (2002), which described the isotopic composition of precipitation as a function of the absolute value of station latitude (LAT) and altitude (ALT):

$$\delta^{18}O = a|LAT|^2 + b|LAT| + cALT + d \qquad (3)$$

where a, b, c and d were empirical parameters.

We further extended the model by step-by-step regression analysis to account for temperature, altitude, and latitude (TAL model) to determine the spatial variation of $\delta^{18}O_{PPT}$ across China. This model considers the isotopic composition of precipitation as the sum of temperature driven rainout effect and terrain patterns (Bowen and Revenaugh 2003) as follows:

$$\delta^{18}\text{O} = \text{a}T + \text{b}ALT / LAT^2 + \text{c}ALT^{0.5} + \text{d} \qquad (4)$$

We compared the performance of the Farquhar, BW and TAL model in simulating $\delta^{18}O_{PPT}$ across China by the values of Mean Absolute Error (MAE) and R^2.

Based on 126 station residuals from Eq.(4), a 5 km × 5 km grid was interpolated on the ground of China using an inverse-distance-weighted approach to incorporate the combined influence of latitude effect, altitude effect and temperature to reveal the spatial distribution of model residuals across China. We incorporated vapor-transport effects in our best estimate $\delta^{18}O_{PPT}$ map by spatially interpolating the residuals from the altitude, latitude and temperature model and adding those to the map grid generated from the model. To validate the simulations with the TAL model, we compared the simulated $\delta^{18}O_{PPT}$ plus residuals to the newly published precipitation data (Zhang et al. 2017; Wang et al. 2017; Feng et al. 2017).

2 Results

2.1 Observed $\delta^{18}O_{PPT}$

To improve the present empirical model, the correlation relationship of potential describing factors and $\delta^{18}O_{PPT}$ were analyzed (Table 1). The annual average temperature was the most correlative factor correlate of the spatial and temporal variation of $\delta^{18}O_{PPT}$ (P<0.01). The altitude had significantly negative relationship with $\delta^{18}O_{PPT}$ (P<0.01). The annual average humidity had significantly positive relationship with the $\delta^{18}O_{PPT}$ (P<0.01). Latitude had significantly negative effects on the $\delta^{18}O_{PPT}$ (P<0.01). In addition, the annual average precipitation amounts positively correlated with the $\delta^{18}O_{PPT}$ (P<0.05). Although the annual average humidity had a higher influence than the latitude, such dataset were not easy to be obtained compared to the latitude.

$\delta^{18}O_{PPT}$ decrease significantly (R^2=0.07, n=126, P<0.05) towards higher latitudes (-0.11 ‰/°North) (Figure 2a), while $\delta^{18}O_{PPT}$ did not correlate significantly (R^2=0.03, P > 0.05) with longitude (0.04 ‰/°East) (Figure 2b). The spatial variability of $\delta^{18}O_{PPT}$ was strongly correlated with altitude (R^2 =0.18, P< 0.01) (Figure 2c) with more depleted values towards higher elevations (laps rate of -1.00 ‰/km). Also, temperature showed a significant correlation (R^2=0.33) with $\delta^{18}O_{PPT}$ getting more enriched towards higher temperature (0.24 ‰/°C) (Figure 2d).

2.2 Simulated $\delta^{18}O_{PPT}$

The Farquhar model to simulate $\delta^{18}O_{PPT}$ as a function of temperature, precipitation amount and altitude across China based on 126 stations was described as follows

$$\delta^{18}\text{O} = 0.35T - 0.004T^2 - 0.004PPT + 1.52\text{E}^{-6}PPT^2 - 0.02ALT^{0.5} - 9.74$$

$$(R^2=0.31, P<0.001) \qquad (5)$$

The coefficients of these models were re-fitted

Table 1 Correlation coefficients matrix of precipitation oxygen-18 isotope and affecting factors in China

	Oxygen-18 (‰)	Latitude (°)	Longitude (°)	Altitude (m)	AAPA (mm)	AAT (°C)	AAWS (m/s)	AAH (%)
Oxygen-18 (‰)	1							
Latitude (°)	-0.235**	1						
Longitude (°)	0.077	-0.173	1					
Altitude (m)	-0.399**	-0.015	-0.422**	1				
AAPA (mm)	0.222*	-0.741**	0.431**	-0.372**	1			
AAT (°C)	0.452**	-0.611**	0.363**	0.644**	0.679**	1		
AAWS (m/s)	-0.158	0.198*	0.053	0.061	-0.043	-0.238**	1	
AAH (%)	0.248**	-0.521**	0.386**	-0.535**	0.744**	0.601**	-0.185*	1

Note: **means significance at 0.01 level, * means significance at 0.05 level;
AAPA means annual average precipitation amount; AAT means annual average temperature; AAWS means average wind speed; AAH means annual average humidity.

Table 2 Comparison of three empirical models for isotope modelling in precipitation.

Model	Equation	Parameters	R^2	Residual sum of squares
Farquhar	$\delta^{18}O=aT+bT^2+cPPT+dPPT^2+eALT^{0.5}+f$	0.35, -0.004, -0.004, 1.52E-6, -0.02, -9.74	0.31	682.31
BW	$\delta^{18}O=a\|LAT\|^2+ b\|LAT\|+cALT+d$	-0.02, 0.90, -0.001, -19.62	0.30	693.02
TAL	$\delta^{18}O=aT+bALT/LAT^2+cALT^{0.5}+d$	0.31, -1.74, 0.11, -13.07	0.46	583.69

Note: BW model is Bowen & Wilkinson Model, TAL model is a Temperature, Altitude and Latitude model.

to this Chinese dataset. Thus, the Farquhar model could explain about 31.3% of the spatial variability of observed $\delta^{18}O_{PPT}$ across China. The relationship between modeled and observed values was linear with a slope of 1, and intercept of 0.0. The mean absolute error between observed $\delta^{18}O_{PPT}$ values and estimated with the Farquhar model was 1.81‰ (σ=1.43).

The BW model to simulate $\delta^{18}O_{PPT}$ as a function of latitude and altitude across China based on 126 stations read as follows

$$\delta^{18}O = -0.02|LAT|^2 + 0.90|LAT| - 0.001ALT - 19.62 \quad (R^2=0.30, P<0.001) \quad (6)$$

Thus, the BW model could explain about 30.4% of the spatial variability of observed $\delta^{18}O_{PPT}$ across China. The relationship between modeled and observed values was linear with a slope of 1.01, an intercept of 0.27. The mean absolute error between observed $\delta^{18}O_{PPT}$ values and estimated with the BW model was 2.13‰ (σ=1.72).

The TAL model for $\delta^{18}O_{PPT}$ simulation resulted in the following relationship:

$$\delta^{18}O = 0.31T - 1.74ALT / LAT^{\wedge 2} + 0.11ALT^{0.5} - 13.07 \quad (R^2=0.46, P<0.001) \quad (7)$$

All the parameters showed significance ($P<0.001$). Thus, the TAL model could explain about 46.3% of the spatial variability of $\delta^{18}O_{PPT}$ across China. The modeled isotopes in precipitation were significantly different to the values of Farquhar and BW models ($P<0.05$). The relationship between modeled and observed values was linear with a slope of 1.02, an intercept of 0.15. Given the presented database, the MAE between observed and simulated $\delta^{18}O_{PPT}$ values was 1.51‰ (σ=1.12). Table 2 reports the parameter estimates, R^2 and F values for the three models. The performance of the TAL model was better than the Farquhar and BW models in China where the altitude ranged from 3 to 5200 m a.s.l. in the given dataset.

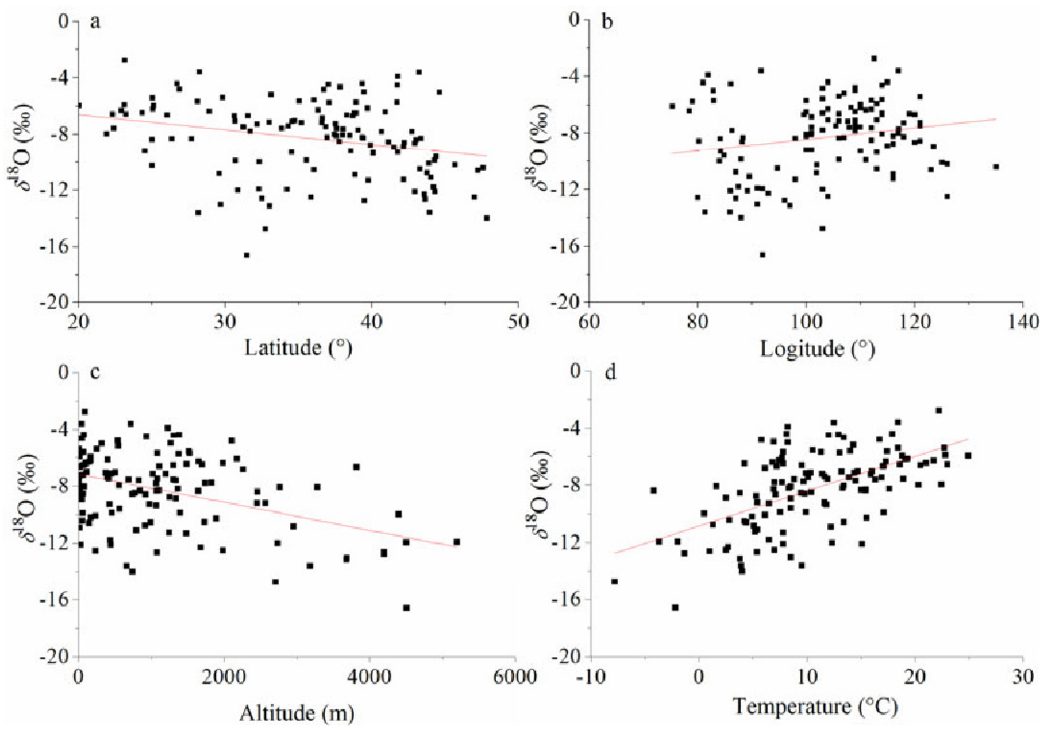

Figure 2 The linear regression of latitude (a), longitude (b), altitude (c) and temperature (d) vs. $\delta^{18}O_{PPT}$ in China.

2.3 Spatial distribution of model residuals in China

Following comparison of interpolation schemes, the provided dataset and the TAL model (which proved to provide the best estimates) were used to generate national precipitation $\delta^{18}O_{PPT}$ grids. The residuals describing the difference between observed value and those predicted values by the TAL model are shown in Figure 3. Difference between estimated and observed $\delta^{18}O_{PPT}$ ranged from -5.27‰ to 4.25‰. 61.9% of the residuals in China ranged from to -1.70‰ to 1.80‰, which shows the good performance of the TAL model applied to China. In the Northeast and central and southwest region of China, low-magnitude residuals confirmed that the $\delta^{18}O_{PPT}$ was primarily dependent on altitude, latitude and temperature variations. Biased positive residuals occurred at the western Tibetan Plateau and northern Mongolia Plateau. The model underestimated $\delta^{18}O_{PPT}$ values in these regions. On the contrary, the TAL model overestimated $\delta^{18}O_{PPT}$ over the northern of Xinjiang within a relatively small area. Residual reflected that the importance of other factors such as continental effect, precipitation amount effect, moisture transport trajectory and relative humidity influence $\delta^{18}O_{PPT}$ distribution.

To assess the effects of altitude on the model performance, the linear regression was conducted between altitude and residuals (Figure 4). There was no significant relationship between model residuals and altitude. The regression slope was 5.56E^{-05} and R was 0.03. These results indicated that the performance of this new model was not affected by the altitude.

2.4 Spatial distribution of $\delta^{18}O_{PPT}$ across China

The spatial distribution of annual $\delta^{18}O_{PPT}$ values in the precipitation by the TAL model across China is shown in Figure 5. The latitude, altitude and temperature dependence of $\delta^{18}O_{PPT}$ and regional deviation thereof were accounted for in this map. The map reproduces $\delta^{18}O_{PPT}$ closely, with a MAE of 0.07‰ (σ=0.87%, n=126). The relationship between simulated $\delta^{18}O_{PPT}$ with residuals and measurements was linear with a slope of 0.98 and R^2=0.95.

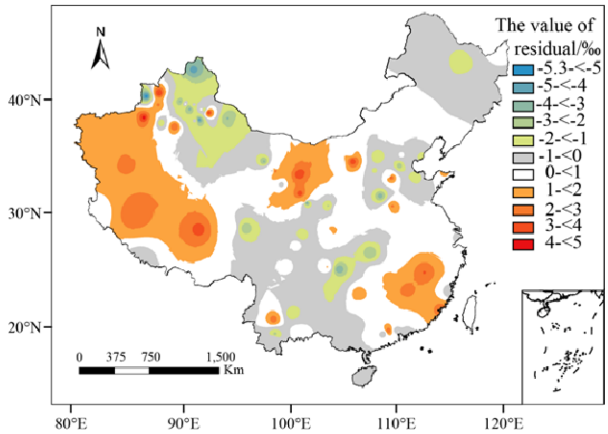

Figure 3 The residual error (observed–simulated) of the TAL model in China. (TAL model is a model improved by us to account for temperature, altitude, and latitude).

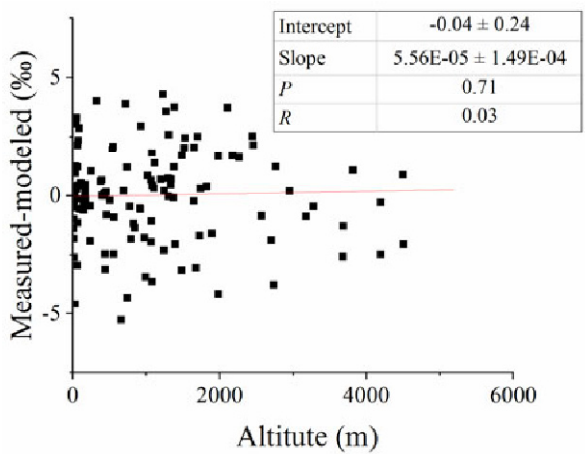

Figure 4 The regression analysis of altitude and TAL model residuals in China. (TAL model is a model improved by us to account for temperature, altitude, and latitude).

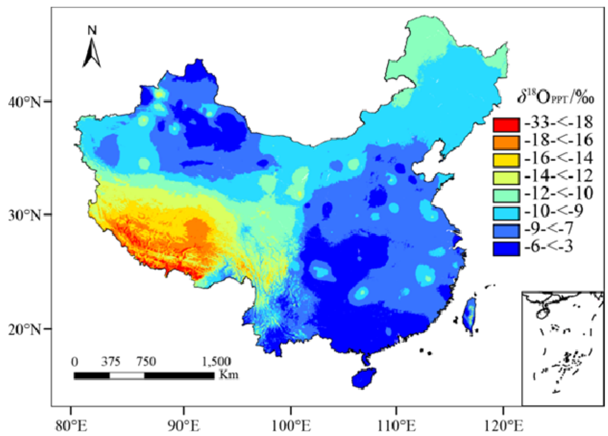

Figure 5 The national wide distribution map of annual mean $\delta^{18}O_{PPT}$ in China.

$\delta^{18}O_{PPT}$ decreased from the low latitudes toward the high latitudes and from low altitudes towards high altitude area. For example, precipitation in northeast of China had low $\delta^{18}O_{PPT}$ values, while they were highest in the southern coast. On the contrary, the Himalaya Mountains had the lowest $\delta^{18}O_{PPT}$. While in the Tibetan plateau, pronounced low $\delta^{18}O_{PPT}$ values were found, which is mainly attributed to strong altitude effect. The effect of altitude on the spatial distribution of $\delta^{18}O_{PPT}$ was very clear for the Qinghai-Tibet plateau, the Tianshan Mountains and the Altai Mountains area.

The validation with recently published data that was not used in the calibration confirmed the high predictivity of the model. Estimated $\delta^{18}O_{PPT}$ values at Anqing (117.07°E, 30.51°N) was -7.54‰, compared to the measured value of -7.23‰ (Zhang et al. 2017). At Pailugou (100.28°E, 38.53°N), the simulated $\delta^{18}O_{PPT}$ value was -9.70‰, while the measured value was -9.07‰ (Feng et al. 2017). $\delta^{18}O_{PPT}$ simulation for Weinan (109.46°E, 34.49°N) was -7.35‰, which was close to the measured value of -7.28‰ (Wang et al. 2017). In each case, the simulated $\delta^{18}O_{PPT}$ maps closely approximated the measurements. In addition, the Equation (7) showed that a temperature increase by 1°C would lead to an average $\delta^{18}O_{PPT}$ enrichment of 0.31‰ for China. This value was closely to the linear regression of the $\delta^{18}O_{PPT}$ and temperature (0.24‰).

3 Discussion

3.1 Model performance

Comparison of three models for the spatial interpolation of precipitation $\delta^{18}O_{PPT}$ showed that the proposed TAL model including temperature as a variable performed better than the Farquhar model, which was limited to altitude, temperature and precipitation amount as variables and BW model, which was limited to altitude and latitude as variables. In addition, the residuals did not show a significant linear relationship with altitude. The residuals of BW model showed significantly linear relationship with the altitude at global scale (Bowen & Wilkinson 2002) and national scale (e.g. China in Liu et al. 2008). Bowen (2010) argued that, the processes correlated of the spatial distribution of $\delta^{18}O_{PPT}$ can be investigated using such a regression model. More importantly, the TAL model can account for the effect of temperature on the distribution of $\delta^{18}O_{PPT}$, which means the $\delta^{18}O_{PPT}$ map is dynamically following the temperature trend across space. Other research also reflects the importance of temperature to influence $\delta^{18}O_{PPT}$ (Dutton et al. 2005). Reiteration of the procedure here, for paleo-$\delta^{18}O_{PPT}$ data, may illuminate past changes in the hydrological cycle and physical parameters controlling the distribution of $\delta^{18}O_{PPT}$ regimes.

This regression model attempts to derive explicit relationships between isotopic composition and parameters that describe mechanistic relationships to isotope values. Our model suggests that precipitation isotope ratios decrease with decreasing temperature, increasing altitude, and increasing latitude, consistent with observed patterns in global datasets (Dansgaard 1964; Rozanski et al. 1992). These ancillary parameters are better and easier sampled (e.g., known at more sites or more accurately or more cheaply or longer time series than isotopes) and could according to our model provide a basis for extrapolating precipitation isotopic ratio variation to unmonitored locations.

3.2 Spatial distribution of $\delta^{18}O_{PPT}$ in China

Based on the data from 126 stations, the spatial distribution of stations was less variable than that in the former study (e.g., Liu et al. 2008). In general, the presented pattern of $\delta^{18}O_{PPT}$ distribution was similar to that previously documented, but with considerable refinement. This spatial patterns of $\delta^{18}O_{PPT}$ depicted in the map over China reflects meridional, altitudinal, and continental temperature effects. The resulted map included modeling values for sites far from monitoring stations as well as fine-scale variation related to topography. The map played an important role in the identification and characterization of meaningful and useful patterns of isotope variation on a regional scale (Rozanski et al. 1992). Large scale of atmospheric vapor transport also affected $\delta^{18}O_{PPT}$ by changing the length and origin of vapor-transport pathway (Boyle 1997). These effects appeared as regional deviation of observed stations from the prediction with the presented TAL model. The vapor transport effect in the best estimated $\delta^{18}O_{PPT}$ map were incorporated by spatial interpolating the residuals from the latitude, altitude and temperature model and adding those to the map grid generated from the model.

Broad regions across the China, particularly the Tibet Plateau and the western China, exhibited significant differences between observed and modeled values. These differences suggested that caution should be made when using the map in those regions. The modeled results were lower than the measured values, which may be related to strong monsoon activities during the period of strong convective precipitation process (Liu et al. 2008). It was the unique topography of the Tibetan Plateau that made the water source of precipitation more complex due to the existence of monsoon and non-monsoon regions (Li et al. 2012). In the southwest monsoon period, water vapor from the Indian Ocean results in low $\delta^{18}O_{PPT}$ (Tian et al. 2001). In other periods, relatively high $\delta^{18}O$ still existed in precipitation, which may cause from recycling of local vapor (Yu et al. 2009). In northwest China, the western region of Xinjiang, the modeled results were obviously higher than the measured values, which may relate to the water vapor in these areas coming from inland re-cycling of precipitation. The precipitation produced by dry continental air often enriched in $\delta^{18}O$ and the strong evaporation also aggravated the enrichment of $\delta^{18}O$ during the raining process.

Generally, with increasing latitude, $\delta^{18}O_{PPT}$ gradually decreased from the south coast to northern China, showing the latitudinal effect. This effect was caused by the gradual removal of lighter isotope water from the air masses when it moved from coastline to inland. Higher $\delta^{18}O_{PPT}$ occurred in the south coast and northwest of China, and lower in the northeast of China and Tibetan Plateau. This result was similar to the findings of Liu et al. (1997) and Li et al. (2012). Zhang et al. (2004) reported that the south vapor path (starting from the tropics through the vapor passage in the Yunnan-Guizhou Plateau to the middle and lower reaches of the Yangtze River), the north vapor path (from west China, via north China to Japan under the westerlies) and the plateau vapor path (from South Asia over the Himalayas to the northern Tibetan Plateau) affected the water source of precipitation in China. These water vapor paths resulted in depleted isotope values in the above-mentioned locations. In the arid region of Northwest China, which is beyond the reach of the Indian Ocean monsoon and Pacific monsoon, re-evaporated moisture plays an important role in the atmospheric water source, which leads to higher $\delta^{18}O_{PPT}$.

The TAL model results revealed that a temperature increase by 1 °C would generally enrich $\delta^{18}O_{PPT}$ values by 0.31 ‰ on average over China. This calculation was nearly identical to that derived from the linear regression result (0.24‰/°C) and in previous studies (0.28‰/°C, Rozanski et al. 1992, 0.30‰/°C, Bowen 2008) both in a global scale). Higher temperature enhances the Rayleigh fractionation process. Consequently, this model allowed the predication of the spatial isotopes pattern in precipitation after temperature change.

Bowen & Wilkinson (2002) pointed out that the distribution map of $\delta^{18}O_{PPT}$ at present afforded several potential uses. Considering the map here accounts for the additional effect of local temperature on $\delta^{18}O_{PPT}$ distribution, temporal change in $\delta^{18}O_{PPT}$ at a single location may be better evaluated with reference to map values than former modeled and interpolated estimates. This means that if the future temperature pattern over a region is given, the distribution pattern of $\delta^{18}O_{PPT}$ can also be estimated. Secondly, the map depicts modern, nationally averaged relationships between $\delta^{18}O_{PPT}$ and a number of explicit (latitude, altitude and temperature) and more obscure (vapor sources, storm tracks) geographic variables. This model allowed the assessment of how these geographical and meteorological factors correlate of the spatial distribution of $\delta^{18}O_{PPT}$. Finally, because regions where $\delta^{18}O_{PPT}$ deviates significantly from the global average geographic and meteorological trends may reflect large-scale vapor-transport patterns, recognition of such areas in a dataset for paleo-$\delta^{18}O_{PPT}$ could highlight temporal variations in atmospheric or oceanic circulation in China.

One of the shortcomings of the current generation of empirical models and geostatistical tools for isotope mapping is their inability to provide time-explicit maps such as daily data. In the future, developing technologies for sample collection and analysis and even the remote measurement of vapor isotope ratios may enable more comprehensive sampling of global water isotope distributions (Helliker & Noone 2010).

4 Conclusions

Based on the TAL model and currently existing $\delta^{18}O_{PPT}$ data in precipitation from 126 stations over China, a model of the quantitative relationship between $\delta^{18}O_{PPT}$ and latitude, altitude and temperature was established. Temperature was found to be the most important explanatory variable in this model. In addition, the average effect of temperature on the $\delta^{18}O_{PPT}$ value was 0.31‰/°C. Although there were some deficiencies, a higher-resolution of spatial pattern of annual $\delta^{18}O_{PPT}$ across China was revealed, generally reflecting the detailed $\delta^{18}O_{PPT}$ pattern in China. $\delta^{18}O_{PPT}$ decreased from the low latitudes toward the high latitude and from low altitudes towards high altitude area. As China's altitude varies considerably, the good performance of this model in China may imply that it can be well allied in an even wider region. With improved accuracy, this model can be used to more closely predict and identify changes in hydro-climate, investigate the spatiotemporal dynamics of atmospheric water transport, and reconstruct material origins with reference to both space and time.

Acknowledgments

This work was financially supported by National Natural Science Foundation of China (41790431 and 41471188), the Innovative Talents Promotion Plan in Shaanxi Province (2017-KJXX-74) and the CAS "Light of West China" Program. We would like to thank the editor and anonymous reviewers for their help in improving the manuscript.

References

Bowen GJ, Revenaugh J (2003) Interpolating the isotopic composition of modern meteoric precipitation. Water Resources Research 39(10): 1299. https://doi.org/10.1029/2003WR002086

Bowen GJ, Wilkinson B (2002) Spatial distribution of $\delta^{18}O$ in meteoric precipitation. Geology 30: 315-318. https://doi.org/10.1130/0091-7613(2002)030<0315:SDOOIM>2.0.CO;2

Bowen GJ (2008) Spatial analysis of the intra-annual variation of precipitation isotope ratios and its climatological corollaries. Journal of Geophysical Research: Atmospheres 113(D5): D05113, https://doi.org/10.1029/2007JD009295

Bowen GJ (2010) Statistical and Geostatistical Mapping of Precipitation Water Isotope Ratios. J.B. West et al. (eds.), Isoscapes: Understanding Movement, Pattern, and Process on Earth Through Isotope Mapping. https://doi.org/10.1007/978-90-481-3354-3_7

Boyle EA (1997) Cool tropical temperatures shift the global δ18O-T relationship: An explanation for the ice core δ18O-borehole thermometry conflict? Geophysical Research Letters 24: 273-276. https://doi.org/10.1029/97GL00081

Cai M, Huang Y, Chen M, et al. (2000) A study on hydrogen and oxygen isotopes composition of precipitation in Xiamen. Journal of Oceanography in Taiwan Strait 19(4): 446-453. (In Chinese). https://doi.org/10.1016/j.jenvrad.2008.04.003

Chan WP, Yuan HW, Huang CY, et al. (2012) Regional Scale High Resolution δ18O Prediction in Precipitation Using MODIS EVI. PloS One 7(9): e45496. https://doi.org/10.1371/journal.pone.0045496

Chen F, Zhang M, Ma Q, et al. (2013) Characteristics of δ18O in precipitation and water vapor sources in Lanzhou city and its surrounding area. Environmental Science 34(10): 3755-3763. (In Chinese)

Dansgaard W (1964) Stable isotopes in precipitation. Tellus B: Chemical and Physical Meteorology 16(4): 436-468. https://doi.org/10.3402/tellusa.v16i4.8993

Dutton AR (1995) Groundwater isotopic evidence for paleorecharge in US High Plains aquifers. Quaternary Research 43: 221-231.https://doi.org/10.1006/qres.1995.1022

Dutton AR, Wilkinson BH, Welker JM, et al. (2005) Spatial distribution and seasonal variation in 18O/16O of modern precipitation and river water across the conterminous USA. Hydrological Processes 19(20): 4121-4146. https://doi.org/10.1002/hyp.5876

Farquhar GD, Lloyd J, Taylor JA, et al. (1993) Vegetation effects on the isotope composition of oxygen in atmospheric CO_2. Nature 363(6428): 439. https://doi.org/10.1038/363439a0

Feng F, Feng Q, Liu X, et al. (2017) Characteristics of δ18O and δD in precipitation and moisture sources of Pailugou catchment in the Qilian Mountains. Natural Resources 37(5): 997-1005. (In Chinese)

Fricke HC, O'neil JR (1999) The correlation between 18O/16O ratios of meteoric water and surface temperature: its use in investigating terrestrial climate change over geologic time. Earth and Planetary Science Letters 170: 181-196.

Gao Z (1993) Discussion on feature of isotope component from atmospheric water, ground water and under ground water in Northwest area, China. Acta Geologica Gansu 2(2): 94-101. (In Chinese)

Gat J R, Klein B, Kushniret Y, et al. (2003) Isotope composition of air moisture over the Mediterranean Sea: an index of the air-sea interaction pattern. Tellus B: Chemical and Physical Meteorology 55: 953-965. https://doi.org/10.1016/S0012-821X(99)00105-3

Guo S, Jia D, Wang R, et al. (2015) Analysis of precipitation characteristics of hydrogen and oxygen stable isotope in Zhenglanqi area of Inner Mongolia. China Science Paper 21: 2580-2584. (In Chinese) https://doi.org/10.3969/j.issn.2095-2783

Helliker BR, David N (2010) Novel approaches for monitoring of water vapor isotope ratios: plants, lasers and satellites. Isoscapes Springer Netherlands, 71-88. https://doi.org/10.1007/978-90-481-3354-3_4

Hoffmann G, Heimann M (1997) Water isotope modeling in the Asian monsoon region. Quaternary International 37: 115-128. https://doi.org/10.1016/1040-6182(96)00004-3

Li YJ, Zhang MJ, Wang SJ, et al. (2012) Stable isotope in precipitation in China: A review. Sciences in Cold and Arid Regions 4: 83-90. https://doi.org/10.3724/SP.J.1226.2012.00083

Liu J, Zhao Y, Liu R (1997) Discussion on the stable isotope time-space distribution law of China atmospheric precipitation. Site Investigation Science and Technology 3: 34-39. (In Chinese)
Liu JR, Song XF, Yuan GF, et al. (2007) Stable isotope evidence of vapor sources in summer Monsoonal precipitation over Southern China. Journal of Natural Resources 22(6): 1004-1012. (In Chinese)
Liu ZF, Tian LD, Chai X, et al. (2008) A model-based determination of spatial variation of precipitation δ18O over China. Chemical Geology 249: 203-212. https://doi.org/10.1016/j.chemgeo.2007.12.011
Liu ZF, Tian LD, Yao TD, et al. (2009) Spatial distribution of $\delta^{18}O$ in precipitation over China. Science Bulletin 54: 804-811. (In Chinese)
Liu X, Song X, Xia J, et al. (2007) Characteristics of Hydrogen and oxygen isotopes and preliminary analysis of vapor source for precipitation in Chabagou catchment of the Loess Plateau. Resources Science 29(3): 59-66. (In Chinese)
Lykoudis SP, Argiriou AA (2007) Gridded dataset of the stable isotopic composition of precipitation over the eastern and central Mediterranean. Journal of Geophysic Research 112: D18107. https://doi.org/10.1029/2007JD008472
Ma L, Jilili A, Li YM (2018) Spatial differentiation in stable isotope compositions of surface waters and its environmental significance in the Issyk-Kul Lake region of Central Asia. Journal of Mountain Science 15(2): 254-263. https://doi.org/10.1007/s11629-017-4499-4
Ma Q, Zhang M, Wang S, et al. (2013) Contributions of moisture from local evaporation to precipitations in southeast China based on hydrogen and oxygen isotopes. Progress in Geography 32(11): 1712-1720. https://doi.org/10.11820/dlkxjz.2013.11.014
Pang SG, Zhao SK, Wen R, et al. (2015) Spatial and temporal variation of stable isotopes in precipitation in the Haihe River basin. Chinese Science Bulletin 60: 1218-1226. https://doi.org/10.1360/N972014-01040
Petit JR, Jouzel J, Raynaud D, et al. (1999) Climate and atmospheric history of the past 420,000 years from the Vostok ice core, Antarctica. Nature 399: 429. https://doi.org/10.1038/20859
Rozanski K, Araguas-Araguas L, Gonfiantini R (1992) Relation-between long-term trends of oxygen-18 isotope composition of precipitation and climate. Science 258: 981-985. https://doi.org/10.1126/science.258.5084.981
Rozanski K, Araguás-Araguás L, Gonfiantini R (1993). Isotopic patterns in modern global precipitation. Climate Change in Continental Isotopic Records 78: 1-36. https://doi.org/10.1029/GM078p0001
Salati E, Dall'Olio A, Matsui E, et al. 1979. Recycling of water in the Amazon Basin: an isotopic study. Water Resource Research 15: 1250-1258. https://doi.org/10.1029/WR015i005p01250
Schmidt GA, LeGrande AN, Hoffmann G (2007) Water isotope expressions of intrinsic and forced variability in a coupled ocean-atmosphere model. Journal of Geophysical Research 112: D10103. https://doi.org/10.1029/2006JD007781
Sharp ZD, Cerling TE (1998) Fossil isotope records of seasonal climate and ecology: straight from the horse's mouth. Geology 26: 219-222. https://doi.org/10.1130/0091-7613(1998)026<0219:FIROSC>2.3.CO;2
Tian LD, Yao TD, MacClune K, et al. (2007) Stable isotopic variations in west China: A consideration of moisture sources. Journal of Geophysical Research: Atmospheres 112: D10112. https://doi.org/10.1029/2006JD007718
Tian L, Yao T, Numaguti A, et al. (2001) Stable isotope variations in monsoon precipitation on the Tibetan Plateau. Journal of the Meteorological Society of Japan 79: 959-966. https://doi.org/10.2151/jmsj.79.959
Tian L, Yao T, Schuster PF, et al. (2003) Oxygen-18 concentrations in recent precipitation and ice cores on the tibetan plateau. Journal of Geophysical Research: Atmospheres 108(D9): 4293-4302. https://doi.org/10.1029/2002JD002173
Tu L, Wang H, Feng Y (2004) Research on D and 18O isotope in the precipitation of Guilin. Carsologica Sinica 23(4): 304-309. (In Chinese)
Terzer S, Wassenaar L, Araguás-Araguás L, et al. (2013) Global isoscapes for δ18O and δ2H in precipitation: improved prediction using regionalized climatic regression models. Hydrology and Earth System Sciences 17: 4713-4728. https://doi.org /10.5194/hess-17-4713-2013
U. S. National Geophysical Data Center (1998) ETOPO-5 five minute gridded world elevation. NGDC, Boulder, Colorado, USA. Available online at: http://www.ngdc.noaa.gov/mgg/global/etopo5, accessed on 20 November 2017.
Ufnar DF, González LA, Ludvigson GA, et al. (2004) Evidence for increased latent heat transport during the Cretaceous (Albian) greenhouse warming. Geology 32: 1049-1052. https://doi.org/10.1130/G20828.1
Wang CH, Peng TR (2001) Hydrogen and oxygen isotopic compositions of Taipei precipitation: 1990-1998. West Pacific Earth Science 1(4): 429-442. (in Chinese)
Wang H, Zhang J, Liu Z (2012) Indications of the hydrogen and oxygen isotopes in precipitation for climate change in Huanglong, Sichuan. Carsologica Sinica 31(3): 253-258. (in Chinese)
Wang S, Zhang M, Hughes CE, et al. (2016) Factors controlling stable isotope composition of precipitation in arid conditions: An observation network in the Tianshan Mountains, central Asia. Tellus B: Chemical and Physical Meteorology 68: 26206. https://doi.org/10.3402/tellusb.v68.26206
Wang X, Lu A, Jiang C, et al. (2017) Characteristics of δD and $\delta^{18}O$ in precipitation and moisture origin in Weinan. Journal of Arid Land Resources and Environment 31(8): 122-128. (In Chinese)
Wei K, Lin R (1994) The influence of the monsoon climate on the isotopic composition of precipitation in China. Geochimica 23(1): 33-41. (In Chinese)
West JB, Bowen GJ, Dawson TE, et al. (2010) Isoscapes: Understanding Movement, Pattern, and Process on Earth Through Isotope Mapping. Springer Science+Business Media B.V. https://doi.org/10.1007/978-90-481-3354-37
Wu J, Yang Q, Ding Y, et al. (2011) Variations and simulation of stable isotopes in precipitation in the Heihe River basin. Environmental Science 32(7): 1857-1866. (In Chinese)
Yu W, Ma Y, Sun W, et al. (2009) Climatic significance of $\delta^{18}O$ records from precipitation on the western Tibetan Plateau. Science Bulletin 54: 2732-2741. https://doi.org/10.1007/s11434-009-0495-6
Yang J, Qin X, Wu J, et al. (2014) The application of modified BW method in studying spatial distribution of $\delta^{18}O$ in precipitation over China. Journal of Glaciology and Geocryology 36(6): 1430-1439. (In Chinese)
Zhang B, Xu Q, Jiang C (2017) Characteristics of δD and $\delta^{18}O$ in the Precipitation and Evaporation Sources in Anqing. Scientia Silvae Sinicae 53(12): 20-29. (In Chinese)
Zhao LJ, Yin L, Xiao HL (2011) Isotopic evidence for the moisture origin and composition of surface runoff in the headwaters of the Heihe River basin. Science Bulletin 55(1): 1-13. https://doi.org/10.1007/s11434-010-4278-x
Zhang S (1989) Characteristics of hydrogen-oxygen isotope composition of complementarily atmospheric sedimentation in Shaanxi province. Geology of Shaanxi 7(2): 57-66. (In Chinese)
Zhang X, Liu J, Sun W, et al. (2006) The relationship between stable isotope ratio of oxygen in precipitation and the related meteorological elements in southwest China. Scientia Sinica Terrae 36: 850-859. (In Chinese)
Zhang X, Liu J, Tian L, et al. (2004) Variations of δ^{18} O in Precipitation along Vapor Transport Paths over Asia. Acta Geographica Sinica 5: 699-708. (In Chinese)
Zhang X, Yao T (1994) World spatial characteristics of oxygen isotope ratio in precipitation. Journal of Glaciology and Geocryology 16: 202-210. (In Chinese)
Zhang W, Kang SC, Shen YP, et al. (2017) Response of snow hydrological processes to a changing climate during 1961 to 2016 in the headwater of Irtysh River Basin, Chinese Altai Mountains. Journal of Mountain Science 14(11): 2295-2310. https://doi.org/10.1007/s11629-017-4556-z